Vailable online at www.sciencedirect.com

SciVerse ScienceDirect

Energy Procedia 27 (2012) 88 – 94

Energy Procedia

SiliconPV: April 03-05, 2012, Leuven, Belgium

Improved parameterization of Auger recombination in silicon

A. Richter[a,*] , F. Werner[b], A. Cuevas[c], J. Schmidt[b], S.W. Glunz[a]

[a]*Fraunhofer Institute for Solar Energy Systems (ISE), Heidenhofstr. 2, 79110 Freiburg, Germany*
[b]*Institute for Solar Energy Research Hamelin (ISFH), Am Ohrberg 1, 31860 Emmerthal, Germany*
[c]*Research School of Engineering, The Australian National University, Canberra, ACT 0200, Australia*

Abstract

Accurate modeling of the intrinsic recombination in silicon is important for device simulation as well as for interpreting measured effective carrier lifetime data. In this contribution we study the injection-dependent effective carrier lifetime applying advanced surface passivation techniques based on Al_2O_3 or SiN_x We show that in some cases the measured lifetime data significantly exceeds the previously accepted intrinsic lifetime limit proposed by Kerr and Cuevas [1]. To verify our measurements we independently perform lifetime measurements with different measurement techniques in two different laboratories. Based on effective lifetime measurements we develop an advanced parameterization of the intrinsic lifetime in crystalline silicon at 300 K as a function of the doping density and the injection level, which accounts for Coulomb-enhanced Auger recombination and Coulomb-enhanced radiative recombination.

Keywords: Auger recombination; radiative recombination; crystalline silicon; surface passivation; aluminum oxide

1. Introduction

Auger recombination processes in semiconductors are band-to-band processes where the excess energy – set free during the recombination of an electron and a hole – is transferred to a third charge carrier. As crystalline silicon is an indirect band-gap semiconductor, radiative recombination is strongly suppressed and thus Auger recombination is the dominant intrinsic recombination mechanism over a wide range of dopant concentrations and injection levels, especially for high dopant concentrations or under high injection conditions. Thus, for device simulation and for the interpretation of effective carrier lifetime data, accurate modeling of the Auger recombination as a function of the dopant concentration *and* the excess carrier density is required.

doi:10.1016/j.egypro.2012.07.034

Auger recombination processes in crystalline silicon are rather complex: Besides the purely collisional processes, where the excess energy is either transferred to an electron (*eeh* process) or hole (*ehh* process), the processes can occur with phonon participation or involve impurities [2-4]. Moreover, Auger recombination is influenced by attractive Coulomb interactions of electrons and holes which lead to the formation of excitions. According to the quantum-mechanical theory of Hangleiter and Häcker, this excition formation leads to an increased density of electrons in the vicinity of holes, which consequently increases the Auger recombination [5].

As the charge carriers involved in the Auger processes are traditionally assumed to be non-interacting quasi-free particles [6-8], the recombination rates of the *eeh* and the *ehh* processes are proportional to the involved carrier densities $R_{\mathrm{eeh}} = C_{\mathrm{n}}\, n^2\, p$ and $R_{\mathrm{ehh}} = C_{\mathrm{p}}\, n\, p^2$, where C_{n} and C_{p} are the Auger coefficients. n and p are the electron and hole densities, respectively. To account for the Coulomb-enhanced Auger recombination, C_{n} and C_{p} are multiplied with enhancement factors g_{eeh} and g_{ehh}, respectively [5]. Based on experimental lifetime data, Altermatt *et al.* parameterized the enhancement factors as a function of the dopant concentration and the temperature for *n*-type and *p*-type silicon in low-injection condition using an empirical expression [9]. There are only few parameterizations which model the Auger recombination as a function of dopant concentration *and* the excess carrier density. One of the most widely used parameterization was proposed by Kerr and Cuevas in 2002 [1]. They included the radiative recombination according to Schlangenotto *et al*. [10] in their parameterization, so that the predicted intrinsic lifetime is given by

$$\tau_{\mathrm{intr,Kerr}} = \frac{\Delta n}{np\left(1.8\times10^{-24}\, n_0^{0.65} + 6\times10^{-25}\, p_0^{0.65} + 3\times10^{-27}\,\Delta n^{0.8} + 9.5\times10^{-15}\right)} \qquad (1)$$

Over the last 10 years the silicon surface passivation was improved continuously, particularly aluminum oxide (Al_2O_3) resulted in very low surface recombination velocities below 5 cm/s [11-15]. Recently, several authors have reported effective lifetimes exceeding the intrinsic limit of Kerr's model [12, 16, 17]. This indicates that applying these improved surface passivation layers allow to investigate silicon bulk recombination with an improved precision, and moreover that it is necessary to revise the intrinsic lifetime limit. Meanwhile, also the model of the radiative recombination in silicon [18, 19], as well as lifetime measurement techniques [20-22] were improved. Based on our own lifetime measurements as well as literature lifetime data, we introduce a new parameterization for the intrinsic recombination of *p*-type and *n*-type silicon at 300 K, taking the aforementioned recent improvements into account.

2. Auger recombination in silicon solar cells

To illustrate the influence of Auger recombination on silicon solar cells, we performed PC1D simulations [23] exemplarily for an *n*-type silicon solar cell with front side boron emitter. The simulation was conducted for a 150 µm thick, 1 Ω cm *n*-type silicon base with a shallow industrial boron doped emitter. Figure 1 shows the recombination current density $J_{\mathrm{rec,mpp}}$ at the maximum power point (mpp), separated into the contributions of the different recombination mechanisms. $J_{\mathrm{rec,mpp}}$ was calculated as a function of the effective rear surface recombination velocity $S_{\mathrm{eff,rear}}$. It can be seen, that with decreasing $S_{\mathrm{eff,rear}}$ the contribution of the Auger recombination increases significantly, reaching about 30% of the total $J_{\mathrm{rec,mpp}}$ at $S_{\mathrm{eff,rear}} = 10$ cm/s, while the contribution of the radiative recombination is more than one order of magnitude smaller. By reducing $S_{\mathrm{eff,rear}}$ from 1000 cm/s to 10 cm/s, the minority carrier density in the bulk and in the emitter region is increased by more than one order of magnitude, which consequently

increased the recombination too, in particular for the Auger recombination. This illustrates, that the relevance of the Auger recombination is gaining importance with improving solar cell technology.

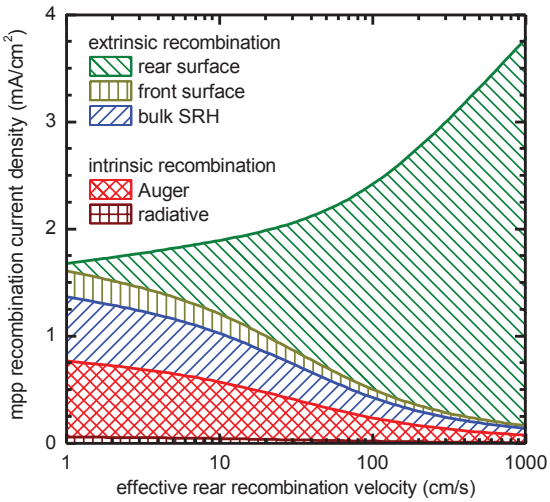

Fig. 1. Recombination current density $J_{rec,mpp}$ at the maximum power point (mpp) as a function of the effective rear recombination velocity. The $J_{rec,mpp}$ is separated into the contribution of each recombination mechanism. The data was simulated using PC1D for an *n*-type silicon solar cell with a 150 µm thick, 1 Ωcm *n*-type silicon base and a shallow industrial boron-doped front side emitter

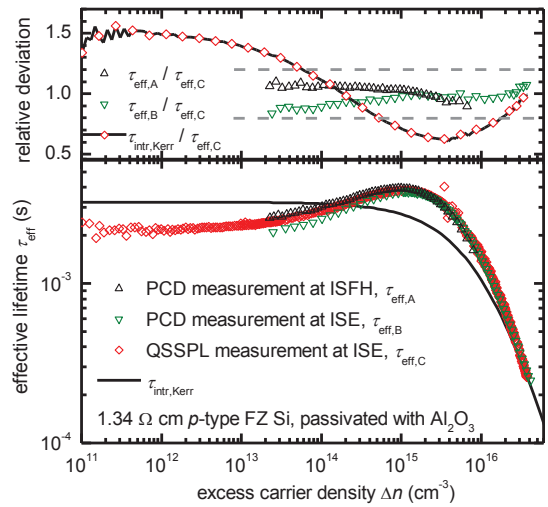

Fig. 2. Comparison of different lifetime measurement techniques at different laboratories. The measurements were performed with an Al_2O_3-passivated 1.34 Ω cm *p*-type FZ Si sample. The solid line represents $\tau_{intr,Kerr}$ after Eq. (1). The upper graph shows the relative deviations of the different τ_{eff} measurements with respect to the QSSPL measurement. The dashed lines mark the estimated uncertainty range of our τ_{eff} measurements

3. Lifetime measurement comparison

As a first step, we verified whether our measured effective lifetime data differs *significantly* from Kerr's intrinsic lifetime limit by comparing different lifetime measurement techniques at two different laboratories: (i) the photo-conductance decay (PCD) [24-26] measurements at ISFH and (ii) PCD as well as quasi-steady-state photo-luminescence (QSSPL) [27] measurements at Fraunhofer ISE. More details about the measurements can be found in Ref. [28]. This is shown exemplarily for a 1.34 Ω cm *p*-type FZ silicon sample passivated with 10 nm ALD Al_2O_3. The resulting effective lifetime data is compared in Fig. 2. The upper graph shows the relative deviation of both PCD measurements with respect to the PL measurement. All measurements are in good agreement, particularly in the Auger recombination-dominated injection range above 5×10^{14} cm^{-3}. It is worth mentioning that this agreement is observed for effective lifetime measurement techniques which are based on completely different physical phenomena: the illumination-induced photo-conductance and photo-luminescence. From these lifetime measurement comparison as well as the measurement uncertainties, we estimated a relative uncertainty range of ±20% for our effective lifetime measurements, which is shown in the upper graph of Fig. 2 as dashed gray lines. Fig. 2 also compares the measured lifetime data with $\tau_{intr,Kerr}$ according to Eq. (1). The relative deviation with respect to the PL measurement is plotted again in the upper graph. For excess carrier densities $\Delta n > 5\times10^{14}$ cm^{-3} $\tau_{intr,Kerr}$ underestimates the measured effective lifetime considerably,

with a maximum relative deviation of 38%. This deviation is clearly higher than our measurement uncertainty of 20% and thus reveals a significant underestimation.

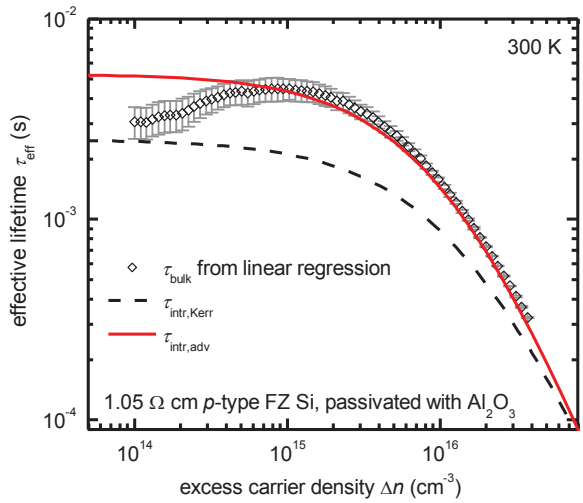

Fig. 3. Bulk lifetime τ_{bulk} of an 1.05 Ω cm *p*-type FZ Si sample passivated with 30 nm Al_2O_3 using plasma-assisted ALD [28]. The bulk lifetime was determined using the wafer thickness variation method. Also plotted are the modeled intrinsic lifetime $\tau_{intr,Kerr}$ according to Eq. (1) and $\tau_{intr,adv}$ according to Eq. (2)

Table I. Parameters for Eq. (2).

param.	unit	Description
n	cm^{-3}	electron density
p	cm^{-3}	hole density
n_0	cm^{-3}	equilibrium electron density
p_0	cm^{-3}	equilibrium hole density
Δn	cm^{-3}	excess carrier density
n_i	cm^{-3}	intrinsic carrier concentration for lowly-doped and lowly-injected silicon, 9.7×10^9 cm^{-3} at 300 K [29]
$n_{i,eff}$	cm^{-3}	effective intrinsic carrier concentration $n_{i,eff} = n_i\, e^{\beta\, \Delta Eg\, /\, 2}$ with the energy band gap narrowing ΔE_g, and $\beta = 1/k_B T$, with the Boltzmann constant k_B and the absolute temperature T
B_{low}	$cm^{-3}s^{-1}$	radiative recombination coefficient for lowly-doped and lowly injected silicon, 4.73×10^{-15} cm^3 s^{-1} at 300 K [18]
B_{rel}	–	relative radiative recombination coefficient, according to Ref. [30]

4. Advanced parameterization of the Auger recombination

We have measured the injection-dependent effective lifetime of high-purity silicon wafers as a function of the dopant concentration of phosphorus-doped *n*-type and boron-doped *p*-type silicon wafers which were passivated with Al_2O_3 or SiN_x. Based on this effective minority carrier lifetime measurements we developed an advanced parameterization of the Auger recombination lifetime as a function of the dopant concentration and the excess carrier density for crystalline silicon at 300 K. We included the radiative recombination according to Refs. [18, 19] which also includes Coulomb-enhanced radiative recombination, thus our parameterization models the complete *intrinsic* recombination:

$$\tau_{intr,adv} = \frac{\Delta n}{\left(np - n_{i,eff}^2\right)\left(2.5\times10^{-31} g_{eeh}\, n_0 + 8.5\times10^{-32} g_{ehh}\, p_0 + 3.0\times10^{-29}\Delta n^{0.92} + B_{rel} B_{low}\right)} \quad (2)$$

with the enhancement factors:

$$g_{eeh}(n_0) = 1 + 13\left\{1 - \tanh\left[\left(\frac{n_0}{N_{0,eeh}}\right)^{0.66}\right]\right\} \text{ and } g_{ehh}(p_0) = 1 + 7.5\left\{1 - \tanh\left[\left(\frac{p_0}{N_{0,ehh}}\right)^{0.63}\right]\right\} \quad (3)$$

with $N_{0,eeh} = 3.3\times10^{17}$ cm^{-3} and $N_{0,ehh} = 7.0\times10^{17}$ cm^{-3}, and with all other parameters specified in Tab. I. We account separately for the Coulomb-enhanced Auger recombination by applying adapted enhancement factorss g_{eeh} and g_{ehh} analogously to those introduced by Altermatt *et al.* [9]. The parameterization provides an excellent accuracy to model the upper limit of the minority carrier lifetime in silicon for the full range of *n*-type and *p*-type dopant densities, as well as a broad range of carrier

injection levels. In the following, the parameterization is exemplarily discussed for *p*-type silicon. A more detailed discussion can be found elsewhere [28], including reasonable simplifications of the parameterization to improve the practical application, particularly concerning the effective intrinsic carrier concentration and the Coulomb-enhanced radiative recombination, which are both rather complex to calculate.

Fig. 3 compares the bulk lifetime τ_{bulk} of an 1.05 Ω cm *p*-type FZ Si sample with the modeled intrinsic lifetime $\tau_{intr,Kerr}$ according to Eq. (1) and $\tau_{intr,adv}$ according to Eq. (2). The bulk lifetime was determined using a wafer thickness variation experiment of mechanically thinned samples [28, 35]. The samples were passivated with 30 nm of Al_2O_3 using plasma-assisted ALD. The experiment reveals a bulk lifetime as high as 4.5±0.5 ms at Δn around 10^{15} cm^{-3} for this 1.05 Ω cm *p*-type FZ Si [28], which is almost twice the 2.3 ms predicted by $\tau_{intr,Kerr}$. As can be seen, our advanced parameterization $\tau_{intr,adv}$ is in excellent agreement with the determined bulk lifetime, in particular in the Auger recombination dominated high injection range.

Fig. 4 shows the maximum measured effective lifetime of our *p*-type samples together with literature data as a function of the dopant concentration. The data is compared to the modeled $\tau_{intr,adv}$ of Eq. (2), the radiative recombination lifetime according to Trupke *et al.* [18], and the Coulomb-enhanced radiative recombination lifetime according to Altermatt *et al.* [30], as well as the free-particle Auger lifetime with Auger coefficients after Dziewior and Schmid [32]. As our prepared lifetime samples cover a dopant concentration range up to N_{dop}= 2×10^{17} cm^{-3}, we used literature data for higher N_{dop} to fit our parameterization. Thus, for N_{dop}>2×10^{18} cm^{-3} $\tau_{intr,adv}$ is in good agreement with the parameterization of Altermatt *et al.* [9] and converges to the free particle Auger lifetime. It can also be seen, that for N_{dop}<10^{16} cm^{-3} the measured effective lifetime is significant below $\tau_{intr,adv}$. This is typically attributed to extrinsic recombination either from the surface or the bulk [9, 28].

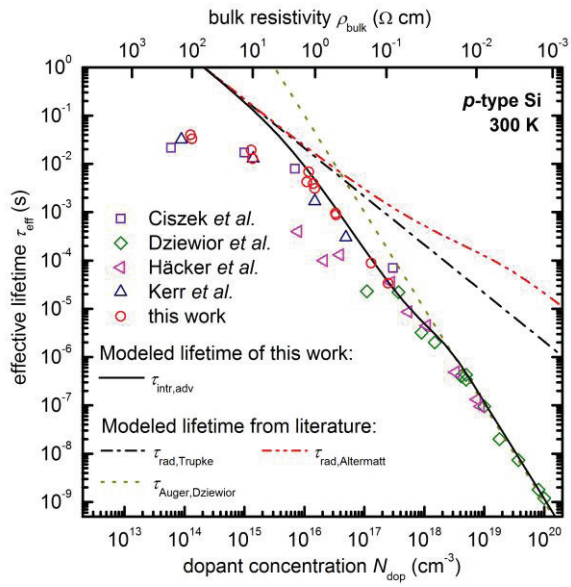

Fig. 4. Maximum effective lifetime as function of the dopant concentration measured at 300 K on *p*-type silicon, together with literature data [31-34]. The data is compared to the modeled $\tau_{intr,adv}$ of Eq. (2). In addition, τ_{rad} according to Trupke *et al.* [18], and according to Altermatt *et al.* [30], as well as the free particle Auger lifetime with Auger coefficients after Dziewior and Schmid [32] is also plotted

5. Summary

Auger recombination can significantly influence the performance of crystalline silicon based solar cells. This is illustrated by PC1D simulations exemplarily for *n*-type silicon solar cells with varying rear side passivation qualities. Recent advances in surface passivation techniques for silicon wafers based on Al_2O_3 have allowed to study silicon bulk recombination with an improved precision. By applying Al_2O_3 passivation layers we found that in some cases the measured effective carrier lifetime exceeds the previously accepted limit for the intrinsic recombination proposed by Kerr and Cuevas [1]. To verify our

measurements we have cross-checked the results with different measurements techniques at two different laboratories. Based on effective lifetime measurements we developed an advanced parameterization of the intrinsic lifetime in crystalline silicon at 300 K which accounts for Coulomb-enhanced Auger recombination and Coulomb-enhanced radiative recombination. This parameterization provides an excellent accuracy for modeling the upper limit of the minority carrier lifetime in crystalline silicon for a wide range of dopant densities, as well as a broad range of carrier injection levels.

Acknowledgements

The authors would like to thank H. Lautenschlager, A. Leimenstoll, and F. Schätzle for wet-chemical wafer treatments, and J. Giesecke for the support with PL measurements. This work has been partially funded by the German Federal Ministry for the Environment, Nature Conservation and Nuclear Safety under contract numbers 0329849A (Th-ETA) and 0325050 (ALD).

References

[1] Kerr MJ and Cuevas A. General parameterization of Auger recombination in crystalline silicon. *J. Appl. Phys.* 2002; 91:2473-80.

[2] Govoni M, Marri I, and Ossicini S. Auger recombination in Si and GaAs semiconductors: *Ab initio* results. *Phys. Rev. B* 2011; 84:075215.

[3] Laks DB, Neumark GF, and Pantelides ST. Accurate interband-Auger-recombination rates in silicon. *Phys. Rev. B* 1990; 42:5176.

[4] Landsberg PT. Trap-Auger recombination in silicon of low carrier densities. *Appl. Phys. Lett.* 1987; 50:745-7.

[5] Hangleiter A and Häcker R. Enhancement of band-to-band Auger recombination by electron-hole correlations. *Phys. Rev. Lett.* 1990; 65:215-18.

[6] Beattie AR and Landsberg PT. Auger effect in semiconductors. *Proc. R. Soc. London A* 1959; 249:16.

[7] Haug A. Carrier density dependence of Auger recombination. *Solid-State Electronics* 1978; 21:1281.

[8] Huldt L. Band-to-band Auger recombination in indirect gap semiconductors. *Phys. Stat. Sol. A* 1971; 8:173.

[9] Altermatt PP, Schmidt J, Heiser G, and Aberle AG. Assessment and parameterisation of Coulomb-enhanced Auger recombination coefficients in lowly injected crystalline silicon. *J. Appl. Phys.* 1997; 82:4938-44.

[10] Schlangenotto H, Maeder H, and Gerlach W. Temperature dependence of the radiative recombination coefficient in silicon. *Phys. Stat. Sol. A* 1974; 21:357-67.

[11] Agostinelli G, et al. Very low surface recombination velocities on p-type silicon wafers passivated with a dielectric with fixed negative charge. . *Sol. Energy Mater. Sol. Cells* 2006; 90:3438-43.

[12] Benick J, Richter A, Hermle M, and Glunz SW. Thermal stability of the Al_2O_3 passivation on p-type silicon surfaces for solar cell application. *Phys. Stat. Sol. RRL* 2009; 3:233-5.

[13] Dingemans G, van de Sanden MCM, and Kessels WMM. Influence of the deposition temperature on the c-Si surface passivation by Al_2O_3 films synthesized by ALD and PECVD. *Electrochem. Solid-State Lett.* 2010; 13:H76.

[14] Hoex B, Heil SBS, Langereis E, van de Sanden MCM, and Kessels WMM. Ultralow surface recombination of c-Si substrates passivated by plasma-assisted atomic layer deposited Al_2O_3. *Appl. Phys. Lett.* 2006; 89:042112.

[15] Schmidt J, Veith B, and Brendel R. Effective surface passivation of crystalline silicon using ultrathin Al_2O_3 films and Al_2O_3/SiN_x stacks. *Phys. Stat. Sol. RRL* 2009; 3:287.

[16] Lüder T, Hahn G, and Terheiden B. Passivation of Si Wafers by ALD-Al_2O_3 Films with Different Surface Conditioning. *Energy Procedia* 2011; 8:660-665.

[17] Suwito D, et al. Detailed study on the passivation mechanism of a-Si_xC_{1-x} for the solar cell rear side. *Proceedings of the 23rd European Photovoltaic Solar Energy Conference*, Valencia, Spain, 2008.

[18] Trupke T, et al. Temperature dependence of the radiative recombination coefficient of intrinsic crystalline silicon. *J. Appl. Phys.* 2003; 94:4930-7.

[19] Altermatt PP, Geelhaar F, Trupke T, Dai X, Neisser A, and Daub E. Injection dependence of spontaneous radiative recombination in crystalline silicon: experimental verification and theoretical analysis. *Appl. Phys. Lett.* 2006; 88:261901-1-3.

[20] Giesecke JA, Niewelt T, Rüdiger M, Schubert MC, and Warta W. Broad range injection-dependent minority carrier lifetime from photoluminescence. *accepted for publication in Sol. Energy Mater. Sol. Cells*.

[21] McIntosh KR, Guo J-H, Abbott MD, and Bardos RA. Calibration of the WCT-100 photoconductance instrument at low conductance. *Prog. Photovolt: Res. Appl.* 2008; 16:279-87.

[22] Trupke T, Bardos RA, and Abbott MD. Self-consistent calibration of photoluminescence and photoconductance lifetime measurements. *Appl. Phys. Lett.* 2005; 87:184102-1- 3.

[23] Clugston DA and Basore PA. PC1D version 5: 32-bit solar cell modeling on personal computers. *Proceedings of the 26th IEEE Photovoltaic Specialists Conference*, Anaheim, California, USA, 1997.

[24] Kane DE and Swanson RM. Measurement of the emitter saturation current by a contactless photoconductivity decay method (silicon solar cells). *Proceedings of the 18th IEEE Photovoltaic Specialists Conference*, Las Vegas, Nevada, USA, 1985.

[25] Nagel H, Berge C, and Aberle AG. Generalized analysis of quasi-steady-state and quasi-transient measurements of carrier lifetimes in semiconductors. *J. Appl. Phys.* 1999; 86:6218- 21.

[26] Sinton RA and Cuevas A. Contactless determination of current-voltage characteristics and minority-carrier lifetimes in semiconductors from quasi-steady-state photoconductance data. *Appl. Phys. Lett.* 1996; 69:2510-2.

[27] Trupke T and Bardos RA. Self-consistent determination of the generation rate from photoconductance measurements. *Appl. Phys. Lett.* 2004; 85:3611-3.

[28] Richter A, Glunz SW, Werner F, Schmidt J, and Cuevas A. *submitted*.

[29] Misiakos K and Tsamakis D. Accurate measurements of the silicon intrinsic carrier density from 78 to 340 K. *J. Appl. Phys.* 1993; 74:3293-7.

[30] Altermatt PP, Geelhaar F, Trupke T, Dai X, Neisser A, and Daub E. Injection dependence of spontaneous radiative recombination in c-Si: experiment, theoretical analysis, and simulation. *Proceedings of the 5th International Conference on Numerical Simulation of Optoelectronic Devices*, Berlin, Germany, 2005.

[31] Ciszek TF and Wang TH. Silicon defect and impurity studies using controlled samples. *Proceedings of the 14th European Photovoltaic Solar Energy Conference*, Barcelona, Spain, 1997.

[32] Dziewior J and Schmid W. Auger coefficients for highly doped and highly excited silicon. *Appl. Phys. Lett.* 1977; 31:346-8.

[33] Häcker R and Hangleiter A. Intrinsic upper limits of the carrier lifetime in silicon. *J. Appl. Phys.* 1994; 75:7570-2.

[34] Kerr MJ and Cuevas A. Very low bulk and surface recombination in oxidized silicon wafers. *Semicond. Sci. Technol.* 2002; 17:35.

[35] Kampwerth H, Rein S, and Glunz SW. Pure experimental determination of surface recombination properties with high reliability. *Proceedings of the 3rd World Conference on Photovoltaic Energy Conversion*, Osaka, Japan, 2003.